British Journal of Mathematics & Computer Science
2(4): 255-280, 2012

SCIENCEDOMAIN *international*
www.sciencedomain.org

On the Stability of a Mathematical Model for Coral Growth in a Tank

L. W. Somathilake[1,2] and J.R. Wedagedera[1,3,4]

[1] *Department of Mathematics, Faculty of Science, University of Ruhuna, Matara, Sri Lanka.*

Research Article

Received: 29 March 2012
Accepted: 09 June 2012
Online Ready: 08 December 2012

Abstract

A mathematical model for coral growth in a well stirred tank is proposed based on nutrient availability. The proposed model is a system of ODEs. Stability analysis of the solutions of the system of ODEs is done for various acceptable parameter regions. Growth forms of corals in different parameter regions are observed based on the solution of the model equations. Numerical calculations and qualitative analysis reveal some interesting global behaviors such as limit cycles, homoclinic connections and heterioclinic connections of the solution trajectories. Unstable growing limit cycles are observed for some parameter values where the corresponding largest limit cycle approaches a homoclinic connection. These behaviors of the solutions of the system closely have biological consequences on coral growth.

Keywords: Coral models, Systems of differential equations, Phase plane analysis, Limit cycles, Local and global stability

2010 Mathematics Subject Classification: 93C15,70K05, 34D20, 34D23

1 Introduction

Coral reefs are made up of a vast amount of calcium carbonate, deposited by colonies of many polyps. Colonies are started when a planktonic coral larva, called a planula, settles on a hard surface. Larva transforms itself into a polyps just after settling [Castro (1997)]. Polyps' maximum diameter is a species specific characteristic. Once they reach this maximum diameter they divide [Merks (2003b)]. In this way, if survive, they divide over and over and form a colony. If the coral colony does not break off it grows as its individual polyps divide to form new polyps [Castro (1997)]. Polyps reside in cups like skeletal structures on stony corals called calices [Merks (2003b)]. As new polyps are formed they build new calices to reside. This cause to growth of the solid matrix of stony corals.

[2] *Corresponding author: E-mail: sthilake@maths.ruh.ac.lk*
[3] *Presently at Department of Mathematics and Statistics, York University, ON M3J 1P3 Canada.*
[4] *E-mail: janakrw@mathstat.yorku.ca*

1.1 Coral Nutrition

Microalgae living inside the coral tissues, zooxanthellae, provides vital nourishment to the coral. Also, small floating animals, zooplankton, and dissolved organic matters are nutritions of corals. Zooxanthellae produce ($C_6H_{12}O_6$) by using sunlight and CO_2 in the sea water and shared it with coral polyps. On the other hand, coral polyps provide shelter to plant tissue. That is there exists a symbiosis relationship between coral polyps and zooxanthellae [Castro (1997); Marineeducation (2012)].

1.2 Growth factors

Structures of the coral colonies of same species can vary with environmental conditions. Growth and morphogenesis of coral depends not only on the type of the coral but also on the environmental conditions: temperature, nutrient availability, calcium carbonate saturation, depth to the reef, light intensity,turbidity, sedimentation,pH and salinity [Mistr (2003); Encyclopedia (2012); Osinga (2011)]. Also same species can exhibit different growth forms under different flow regimes [Mistr (2003)]. Different aspects of coral morphogenesis have been studied using various modelling and computational approaches [Kaandorp (1996, 2005, 2008); Merks (2003a,b,c); Mistr (2003); Maxim (2010)]. Merks has used Diffusion-Limited Aggregation (DLA) approach based on physical mechanisms, diffusion driven instability and Laplacian growth [Merks (2003a)]. Fascinating stony corals like simulations have been reported in [Merks (2003a,b,c); Kaandorp (2005, 2008); Maxim (2010)]. A Reaction-Diffusion-Advection type model for growth of corals has been proposed in [Mistr (2003)].

The aim of this article is to present a hypothetical model for the growth of coral in a tank, considering the interaction between nutrient availability and formation of solid matrix of corals. We proceed to study the stability behavior of the steady states and the global behavior of the solution trajectories of the model equation (system of ODEs). Based on the behavior of solutions of the model some temporal growth forms of the solid are discussed.

The remainder of this article is organized as follows: In section (2), a mathematical model for formation of corals is derived. In sections (3) and (4), the local behavior of the equilibria and global behavior of the solution trajectories in different parameter regions of the model (system of ordinary differential equations) are discussed respectively. Also, the possible growth forms of solid matrix (corals) corresponding to different stability regions are explained.

2 Derivation of the mathematical model

Consider a water filled tank with some coral polyps (coral particles) settled on the bottom of the tank. Assume that nutrients are supplied to the tank in the rate $k(u_s - \bar{u})$; $k > 0$. That is nutrients are supplied to the system if $\bar{u}$ drops below a preassigned value u_s. Since the vessel is well stirred, we can neglect the diffusion of reactants. It is assumed that growth factors except the availability of nutrients are controlled.

Assume that dissolved nutrients react with solid material and produce additional solid material. Let A and B denote the dissolved nutrients and solid material respectively, and $\bar{u}$ and $\bar{v}$ denote their respective concentrations. We simplify the growth process to a hypothetical chemical reaction between A and B of the form:

$$lA + mB \xrightarrow{k_1} nB.$$

Where k_1 is a positive rate constant (reaction rate). l, m and n are the respective stoichiometric constants such that $n = m + l$. Units of k_1 depend on the stoichiometric constants l, m and n.

Consider the case $l = 1$, $m = 2$ and $n = l + m = 3$ as in [Mistr (2003)]. Assume that the solid materials produced by the reaction process deposited by existing coral polyps in the rate $k_2 (> 0)$. Let

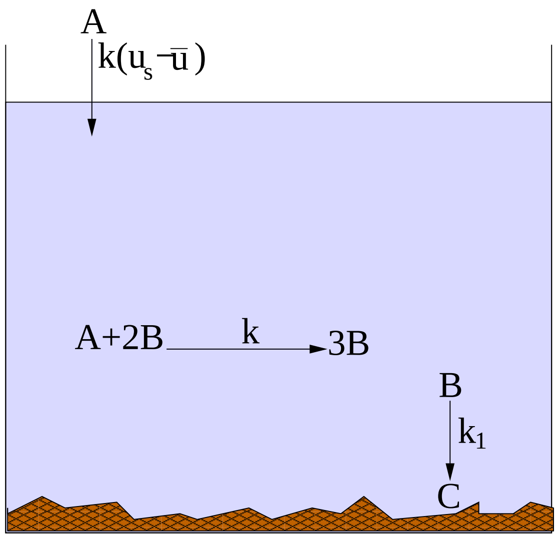

Figure 1: Sketch of the reaction process of the model system

C denotes the solid material concentration deposited by coral polyps. This process can be symbolized as follows:

$$B \xrightarrow{k_2} C. \tag{2.1}$$

Let $\bar{u} = \bar{u}(\tau)$ and $\bar{v} = \bar{v}(\tau)$ be the overall concentrations of reactants (dissolved nutrients and calcium carbonate ions) at time τ. We can immediately write the rate equation for this reaction process as follows:

$$\left(\begin{array}{l} \text{Time rate change of dissolved} \\ \text{nutrient concentration } \bar{u} \end{array} \right) = \left(\begin{array}{l} \text{supplying rate} \\ \text{of } \bar{u} \end{array} \right) - \left(\begin{array}{l} \text{Reactive} \\ \text{loss of } \bar{u} \end{array} \right) \tag{2.2}$$

$$\left(\begin{array}{l} \text{Time rate change of} \\ \text{solid concentration } \bar{v} \end{array} \right) = -\left(\begin{array}{l} \text{loss of of } \bar{v} \\ \text{due to deposition} \end{array} \right) + \left(\begin{array}{l} \text{Reactive production} \\ \text{of } \bar{v} \end{array} \right) \tag{2.3}$$

$$\left(\begin{array}{l} \text{Time rate change of aggregating} \\ \text{solid concentration} \end{array} \right) = \left(\begin{array}{l} \text{depositing solid} \\ \text{concentration} \end{array} \right) \tag{2.4}$$

Where $\bar{w}$ denote the concentration of aggregating solid materials concentration.

By applying the law of mass action [Murray (2003)], these processes can be represented mathematically as follows :

$$\left. \begin{array}{rcl} \frac{d\bar{u}}{d\tau} & = & k(u_s - \bar{u}) - k_1 \bar{u}\bar{v}^2 \\ \frac{d\bar{v}}{d\tau} & = & -k_2 \bar{v} + k_1 \bar{u}\bar{v}^2 \\ \frac{d\bar{w}}{d\tau} & = & k_2 \bar{v} \end{array} \right\}. \tag{2.5}$$

The first, second and third equations of the system (2.5) represent the rate equations (2.2), (2.3) and (2.4) respectively.

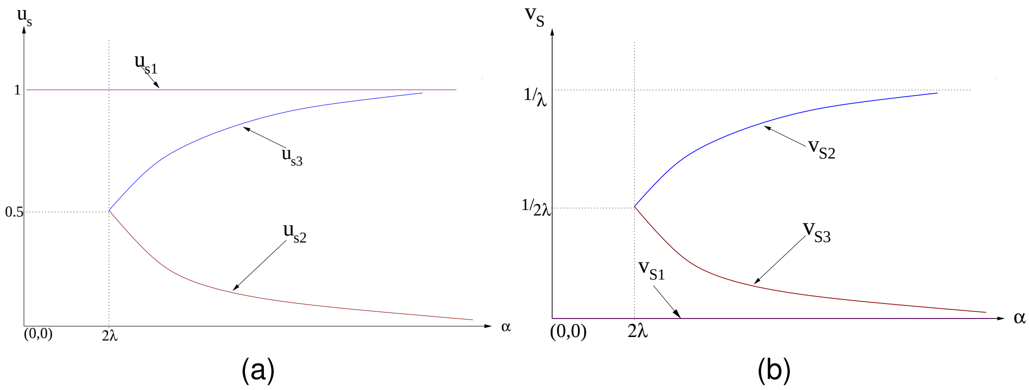

Figure 2: Sketch of the variation of the steady states with respect to α: (a) u_s; (b) v_s.

2.1 Nondimensionalization

The system (2.5) can be nondimensionalized by the substitution $u = \left(\frac{\bar{u}}{u_s}\right)$, $v = \left(\frac{\bar{v}}{u_s}\right)$, $w = \left(\frac{\bar{w}}{u_s}\right)$, $t = k\tau$. By these substitutions the system is reduced to the form:

$$\left.\begin{aligned} \frac{du}{dt} &= 1 - u - \alpha^2 uv^2 \\ \frac{dv}{dt} &= -\lambda v + \alpha^2 uv^2 \\ \frac{dw}{dt} &= \lambda v \end{aligned}\right\}, \tag{2.6}$$

where $\alpha = \frac{k_1 u_s^2}{k}$ and $\lambda = \frac{k_2}{k}$.

3 Local stability of the steady states

Consider the system consisting of first two equations of the model (2.6):

$$\left.\begin{aligned} \frac{du}{dt} &= 1 - u - \alpha^2 uv^2 \\ \frac{dv}{dt} &= -\lambda v + \alpha^2 uv^2 \end{aligned}\right\} \tag{3.1}$$

There are three steady states: $S_1 \equiv (u_{s1}, v_{s1})$, $S_2 \equiv (u_{s2}, v_{s2})$ and $S_3 \equiv (u_{s3}, v_{s3})$, where $u_{s1} = 1$, $v_{s1} = 0$, $u_{s2} = \dfrac{\alpha - \sqrt{\alpha^2 - 4\lambda^2}}{2\alpha}$, $v_{s2} = \dfrac{\alpha + \sqrt{\alpha^2 - 4\lambda^2}}{2\alpha\lambda}$, $u_{s3} = \dfrac{\alpha + \sqrt{\alpha^2 - 4\lambda^2}}{2\alpha}$ and $v_{s3} = \dfrac{\alpha - \sqrt{\alpha^2 - 4\lambda^2}}{2\alpha\lambda}$ for $\alpha > 2\lambda$. For $\alpha = 2\lambda$, S_2 and S_3 coincide each other and for $\alpha < 2\lambda$, only one real steady state, S_1 exists. Let $u_s = \{u_{s1}, u_{s2}, u_{s3}\}$ and $v_s = \{v_{s1}, v_{s2}, v_{s3}\}$ be the steady states of u and v respectively. Then the variation of u_s and v_s with respect to α is shown in Figure (2). In the following sections, the linear stability at the steady states in the cases, $\alpha > 2\lambda$, $\alpha = 2\lambda$ and $\alpha < 2\lambda$ are analyzed separately.

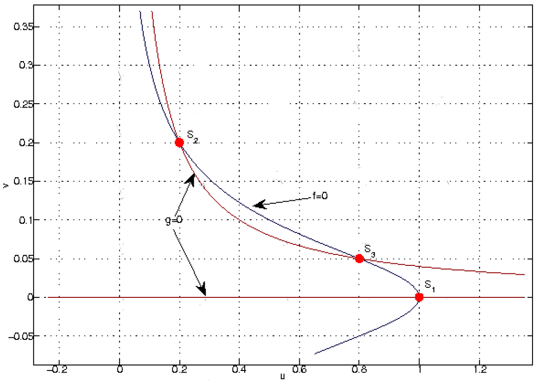

Figure 3: Nullclines and steady states of (3.1) for $\alpha = 10$, $\lambda = 4$ (α and λ lie in parameter region $\alpha > 2\lambda$).

3.1 Case I ($\alpha > 2\lambda$):

The nullclines for particular parameter values in this case are shown in Figure (3). At the trivial steady state S_1 is a nutrient only state. The nontrivial steady states S_2 and S_3 characterize the high and low solid densities (or low and high nutrient concentrations) respectively. In other words, S_2 is "solid dominated" and S_3 is "nutrient dominated" steady states. When there is not enough solid to react, the system reaches S_3 and it reaches S_2 when there is not enough nutrient to react.

The plots of u_s and v_s with respect to α for different values of λ are shown in Figures (4)(a) and (4)(b). As α tends to infinity u_{s2} and u_{s3} reaches 0 and 1 respectively. Similarly, as α tends to infinity v_{s2} and v_{s3} reaches $1/\lambda$ and 0 respectively. In other words, as α tends to infinity $S_3 \longrightarrow S_1$ and $S_2 \longrightarrow (0, 1/\lambda)$ when λ is fixed.

3.1.1 The local stability of equilibrium points via linearizion

We shall now present an overview of the stability of the steady states of the system (3.1). Near the uniform steady state (u_{si}, v_{si}), put $u = u_i + u_{si}$, $v = v_i + v_{si}$ for $i = 1, 2, 3$. Then the linearized systems about (u_{si}, v_{si}), $i = 1, 2, 3$ can be expressed in terms of u_i and v_i of the form:

$$\frac{d\mathbf{u_i}}{dt} = A_i \mathbf{u_i}, \quad i = 1, 2, 3. \tag{3.2}$$

where $\mathbf{u_i} = (u_i, v_i)^T$,

$$A_i = \begin{pmatrix} a_{11} & a_{12} \\ a_{21} & a_{22} \end{pmatrix}\Bigg|_{(u_{si}, v_{si})} = \begin{pmatrix} \dfrac{\partial f}{\partial u} & \dfrac{\partial f}{\partial v} \\ \dfrac{\partial g}{\partial u} & \dfrac{\partial g}{\partial v} \end{pmatrix}\Bigg|_{(u_{si}, v_{si})} = \begin{pmatrix} -1 - \alpha^2 v_{si}^2 & -2\lambda \\ \alpha^2 v_{si}^2 & \lambda \end{pmatrix}; \quad \text{i=1,2,3.}$$

Let $p_i = \mathrm{tr}(A_i)$, $q_i = \det(A_i)$; $(i = 1, 2, 3)$. Then $p_1 = -1 - \lambda$, $p_2 = \lambda - \alpha(\alpha + \sqrt{\alpha^2 - 4\lambda^2})/(2\lambda^2)$, $p_3 = \lambda - \alpha(\alpha - \sqrt{\alpha^2 - 4\lambda^2})/2\lambda^2$, $q_1 = \lambda$, $q_2 = (\alpha^2 - 4\lambda^2 + \alpha\sqrt{\alpha^2 - 4\lambda^2})/2\lambda$ and $q_3 = (\alpha^2 - 4\lambda^2 - \alpha\sqrt{\alpha^2 - 4\lambda^2})/2\lambda$. Also let $\Delta_i = p_i^2 - 4q_i$; $i = 1, 2, 3$. Next the linear stability of the equilibrium points S_i, $(i = 1, 2, 3)$ in the case $\alpha > 2\lambda$ are investigated separately using eigenvalue techniques [Murray (2003); Jordan (1987)].

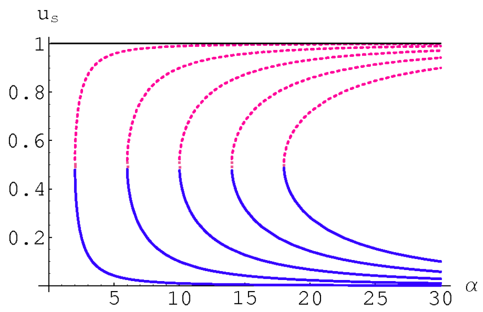

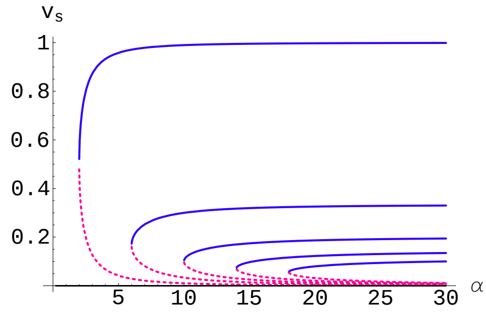

Figure 4: Plots of u_s and v_s for different values of λ (for the left to right curves, values of λ are $1, 3, 5, 7$ and 9 respectively). (a) Solid and dotted curve represent u_{s2} and u_{s3} respectively; horizontal solid line through the point $(0, 1)$ is u_{s1}, (b) Solid and dotted curve represent v_{s2} and v_{s3} respectively; Horizontal solid line (along α axis) is v_{s1}
.

3.1.2 The linear stability of the steady state S_1

The behavior of the steady states are determined by the behavior of the eigenvalues of A_i. Since $p_1 < 0$, $q_1 > 0$ and $\Delta_1 = p_1^2 - 4q_1 = (\lambda - 1)^2 > 0$, we have both eigenvalues of A_1 negative which result a stable node at S_1. That is "nutrient only" steady state is always stable.

3.1.3 The linear stability of the steady state S_2

Solving $p_2 = 0$ for α (i.e. Hopf-bifurcation) we get the solutions: $(p_2)\alpha_1 = \dfrac{\lambda^2}{\sqrt{\lambda - 1}}$ and $(p_2)\alpha_2 = \dfrac{-\lambda^2}{\sqrt{\lambda - 1}}$. Similarly solving $\Delta_2 = 0$ for α we get four solutions two of which are
$(\Delta_2)\alpha_1 = \dfrac{\sqrt{\lambda^3(3\lambda^2 + 7\lambda + 8) + 2\sqrt{2}\sqrt{\lambda^7(\lambda^3 + 3\lambda^2 - 4)}}}{(1 + \lambda)}$ and
$(\Delta_2)\alpha_2 = \dfrac{\sqrt{\lambda^3(3\lambda^2 + 7\lambda + 8) - 2\sqrt{2}\sqrt{\lambda^7(\lambda^3 + 3\lambda^2 - 4)}}}{(1 + \lambda)}$ both are positive and the other two are $-(\Delta_2)\alpha_1$ and $-(\Delta_2)\alpha_2$. Since $\alpha > 2\lambda$ putting $\alpha = 2\lambda + \epsilon$, where $\epsilon > 0$ we have

$$\begin{aligned} p_2 &= -\frac{(2\lambda + \epsilon)^2 - 2\lambda^3 + (\text{positive term})}{2\lambda^2} \\ &= -\frac{2\lambda^2(2 - \lambda) + (\text{positive term})}{2\lambda^2} \\ &< 0; \quad \text{if } \lambda < 2. \end{aligned} \tag{3.3}$$

Therefore p_2 is negative for $\lambda < 2$. The region determined by $\alpha > 2\lambda$ of the positive quadrant of the (α, λ) parameter space can be divided in to four subregions(See Figure (5)) :

Region I : $2\lambda < \alpha < (\Delta_2)\alpha_1$, $\lambda > 2$;

Region II: $(\Delta_2)\alpha_1 < \alpha < (p_2)\alpha_1$, $\lambda > 2$;

Region III: $(p_2)\alpha_1 < \alpha < (\Delta_2)\alpha_2$, $\lambda > 1$ and

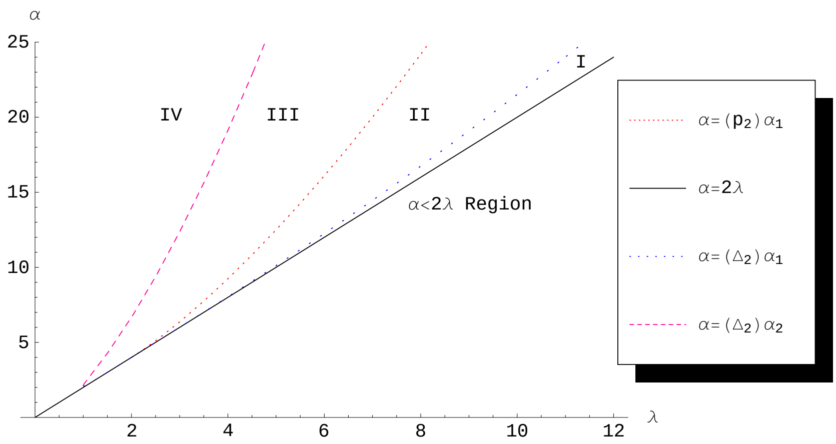

Figure 5: Parameter regions depending on the type of equilibria of S_2.

Region IV: $(\Delta_2)\alpha_2 < \alpha$, $\lambda > 0$.

Now using the Eigenvalues interpretation of the classification of equilibrium points, the behavior of S_2 in regions I, II, III and IV can be classified as in the Table 1.

Region	p_2	q_2	Δ_2	Type of the equalibria
I	positive	positive	positive	Unstable nodes
II	positive	positive	negative	Unstable spirals
III	negative	positive	negative	Stable spirals
IV	negative	positive	positive	Stable nodes

Table 1: Classification of the equilibria S_2 in different parameter regions

The behavior of the steady state S_2 depends on the parameters λ and α. The curve $\alpha = (p_2)\alpha_2$ bifurcates the steady state S_2 into *unstable-stable* spirals. The curve $\alpha = (\Delta_2)\alpha_1$ bifurcates S_2 into unstable *node-spirals* and $\alpha = (\Delta_2)(\alpha_2)$ bifurcate S_2 into stable *spiral-node*.

Also, on the curve $(p_2)\alpha = \frac{\lambda^2}{\sqrt{\lambda - 1}}$, p_2 is zero and $\Delta_2 < 0$ and hence the steady state S_2 is a center. On the line $\alpha = 2\lambda$ the local behavior of the steady state S_2 (In this case S_2 and S_3 are coincide) is indeterminate.

3.1.4 The linear stability of the steady state S_3

It is not difficult to see that $q_3 < 0$, in the region $\alpha > 2\lambda$. Therefore, this steady state is a saddle for all the parameter values in the region $\alpha > 2\lambda$. That is 'nutrient dominated" steady state is always a saddle.

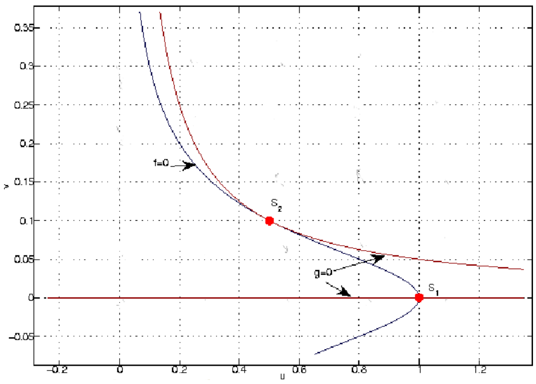

Figure 6: Nullclines on parameter line $\alpha = 2\lambda$ (for $\alpha = 10$, $\lambda = 5$)

3.2 Case II: $\alpha = 2\lambda$

On the line $\alpha = 2\lambda$, the number of equilibrium points reduce to two and these points are $S_1 \equiv (1, 0)$ and $S_2 \equiv (\frac{1}{2}, \frac{1}{2\lambda})$. The nullclines for particular parameter values in this case are shown in Figure (6). In this case, at the point S_2, $p_2 = \lambda - 2$, and $q_2 = 0$. Therefore, the type of the stability is indeterminate. In this case all the trajectories except the stable trajectories at S_2 reach S_1.

3.3 Case III: $\alpha < 2\lambda$

In this case only one steady state, $S_1 \equiv (0, 1)$, exists. The nullclines and phase plane diagram for this case are shown in Figures (7)(a) and (7)(b) respectively. The steady state S_1 is a stable node. There are no other steady states and so, S_1 is globally stable. All the trajectories in phase plane tend to this nutrient only steady state S_1. That is, if the system starts at any state (that is whatever the starting state) solid particles condensate more rapidly than that produce by the reaction. Therefore, the solid, that remain to the reaction process get vanished. Therefore, growth of solid can be expected until the system stabilize at S_1. After that the growth ceases.

4 The structure of the trajectories in a region containing all the steady states(Global behavior)

In this section, the global behavior of the trajectories are discussed in each parameter region separately. Furthermore, some behavioral structures of the solutions in different parameter regions are presented.

Corollary 4.0.1. *When $\alpha > 2\lambda$, the steady states S_1, S_2 and S_3 lie on the line*

$$l \equiv v - \frac{1}{\lambda}(1 - u) = 0. \tag{4.1}$$

Proof. It can easily be shown that the coordinates of the points S_1, S_2 and S_3 satisfy the equation of the given line by direct substitution. ☐

Theorem 4.1. *There exist confined sets containing S_1, S_2 and S_3 when $\lambda > 1$.*

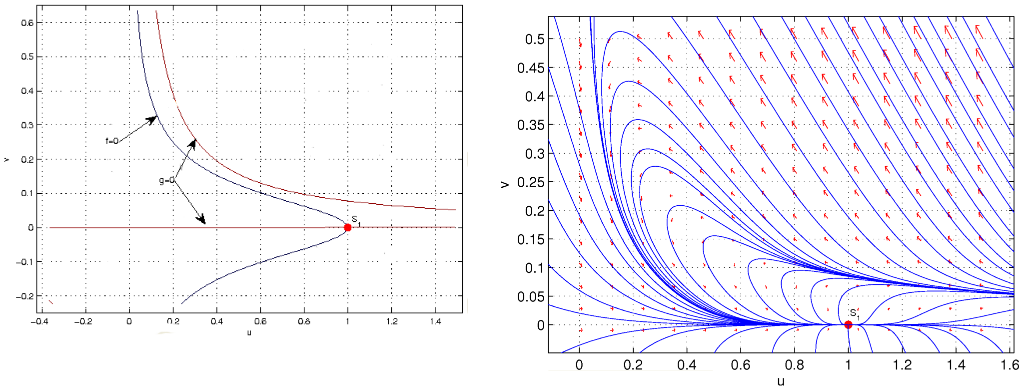

(a) (b)

Figure 7: (a) nullclines and (b) phase plane diagram in parameter region $\alpha < 2\lambda$ (for $\alpha = 8$, $\lambda = 5$)

Proof. Consider the region $\mathcal{R}$ shown in Figure (8)(a). Where $l_2 \equiv v - m(1-u) = 0$. Now we check the existence of positive values of m such that all the trajectories passing through l_2 directed inwards to the region $\mathcal{R}$. That is, we have to check the existence of positive values for m such that $\left.\dfrac{dv}{du}\right|_{l_2} < -m$.

$$\begin{aligned}\left.\frac{dv}{du}\right|_{l_2} < -m \quad &\Rightarrow \frac{-\lambda m(1-u) + \alpha^2 m^2 u(1-u)^2}{1-u-\alpha^2 m^2 u(1-u)^2} < -m \\ &\Rightarrow \alpha^2 m u(1-u)^2(m-1) + (1-u)(\lambda - 1) > 0\end{aligned} \tag{4.2}$$

The inequality (4.2) holds for all $m > 1$ when $0 < u < 1$. As we have shown in Corollary (4.0.1); S_1, S_2 and S_3 lies on the line $l_1 \equiv \lambda v - (1-u)$. Also the gradient of l_1 is $-\dfrac{1}{\lambda}$ and it satisfies the inequality $-\dfrac{1}{\lambda} > -1 > -m$ for $\lambda > 1$. These facts confirm that S_1, S_2 and S_3 lie in the chosen area $\mathcal{R}$. Now, consider the behavior of the trajectories on the each side of the region $\mathcal{R}$.

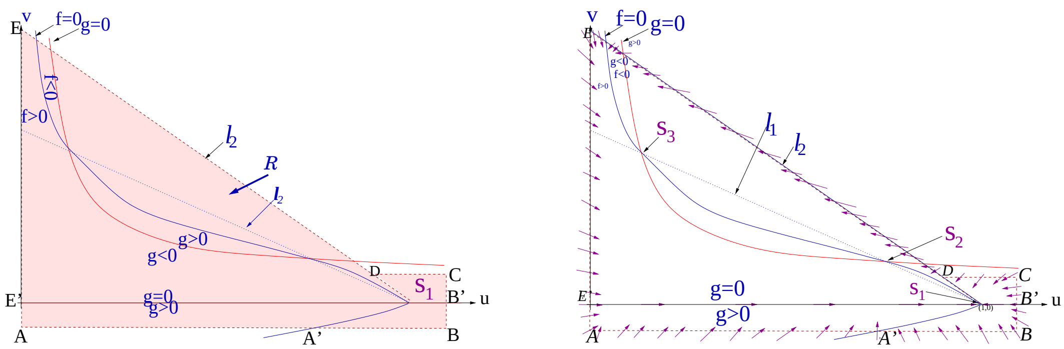

(a) (b)

Figure 8: (a)The region $\mathcal{R}$; (b) A confined set containing S_1, S_2 and S_3

On AB: On the section AA', $f > 0$ and $g > 0$. Therefore, on this section trajectories are pointed inwards the region $\mathcal{R}$. Also on $A'B$, $f < 0$ and $g > 0$ and trajectories are pointed inwards the domain as shown in the Figure (8)(b).

On BC: On BB', $f < 0$ and $g > 0$ and on $B'C$, $f < 0$ and $g < 0$. Therefore, on both of the section trajectories are pointed inwards the region $\mathcal{R}$.

On CD: On this line, $f < 0$ and $g < 0$ and hence trajectories are pointed inwards the region.

On DE: On this section, trajectories are pointed inwards of the region since we have chosen m satisfying this condition.

On EA: On the line EE', $f > 0$ and $g < 0$ as well as on section $E'A$, $f > 0$ and $g > 0$. Therefore, on both of these line segments trajectories are pointed inwards the domain as shown in the figure.

Therefore trajectories at each point on the boundary of the region $\mathcal{R}$, are pointed inwards of the region $\mathcal{R}$. Therefore the region $\mathcal{R}$ is a confined set. □

Now we investigate the behavior of the trajectories in the confined set $\mathcal{R}$ when parameters α and λ are in parameter regions I, II, III and IV respectively. The interpretations of the behaviors of the trajectories are based on the Poincarè-Bendixson theorem [Jordan (1987)], which says that any trajectory entering into the confined set $\mathcal{R}$, approaches to a stable point or to a limit cycle.

4.1 Heterioclinic connections and phase diagram in parameter regions I and II

Any trajectory entering into the region $\mathcal{R}$ approaches to S_1, S_3 (only through the two stable trajectories) or a limit cycle.

Theorem 4.2. *For α and λ in regions I and II (sufficiently away from the Hopf bifurcation line), there are three heterioclinic connections, two of which are between S_3 and S_1, and the other one between S_2 and S_3.*

Proof. Consider the two unstable trajectories emerging from the saddle point S_3. These two trajectories do not leave the confined set $\mathcal{R}$ and do not reach S_2 because S_2 is unstable (unstable node or unstable spiral). Also these two trajectories do not reach a limit cycle because there is no limit cycle sufficiently away from the Hopf-bifurcation line. Therefore, these unstable trajectories should reach the stable steady state S_1.

Now consider the two stable trajectories at S_3. One of them emerges from $(\infty, 0)$ and the other trajectory should start from S_2. That is there is a heteroclinic connection between S_2 and S_3. □

The behaviors of these heterioclinic connections are shown in Figure (9). The phase diagrams for particular parameter values in region I and II are shown in Figure (10). The phase diagrams (Figures (10)(a) and (10)(b)) show that all the trajectories, except the two stable trajectories at S_3, reach the trivial steady state S_1. This suggests that small perturbations of steady state S_2 may cause the system to reach S_1 and there is only one path available for the system to reach S_3.

Physical interpretation: In these regions, condensation speed of solid material is higher than the reactive production speed. Hence as time passes the amount of solid material which left to react with nutrient reaches v_{s3} or v_{s1}.

The condensing solid concentration w and v satisfy the differential equation $\frac{dw}{dt} = k_1 v$. Therefore, if the system comes to stabilization (u_s, v_s) at time $t = t_s$, then $w = k_1 v_s \tau + C$ at $t = t_s + \tau$, where C is a constant. Therefore, if the system comes to stabilization (u_s, v_s) and if $v_s \neq 0$, then the condensed solid (coral) concentration grows uniformly. That is if the system comes to stabilization S_3

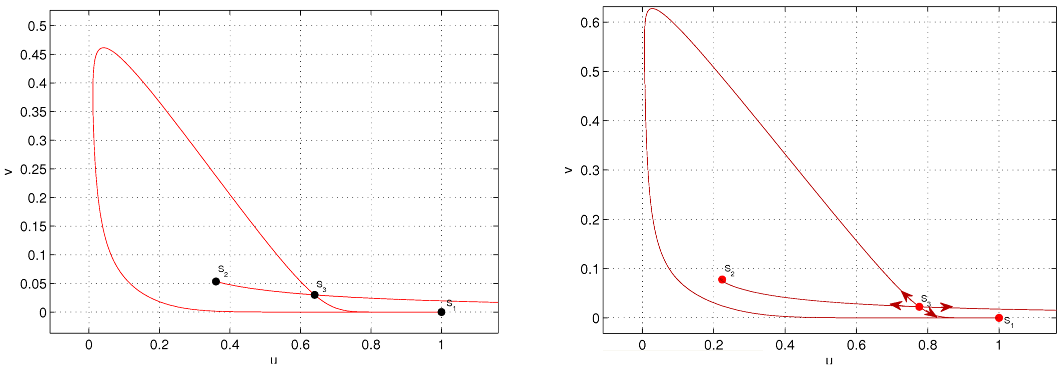

(a) (b)

Figure 9: Stable and unstable trajectories starting at S_3: (a) in parameter region I for $\alpha = 25$, $\lambda = 12$, (b) in parameter region II for $\alpha = 24$, $\lambda = 10$.

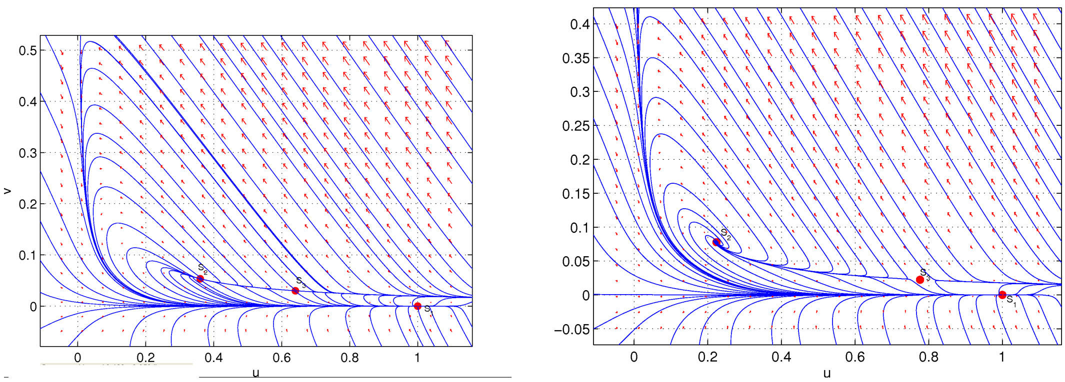

(a) (b)

Figure 10: A phase plane diagram (a) in parameter region I for $\lambda = 12$, $\alpha = 25$; (b) in parameter region II for $\lambda = 10$, $\alpha = 24$.

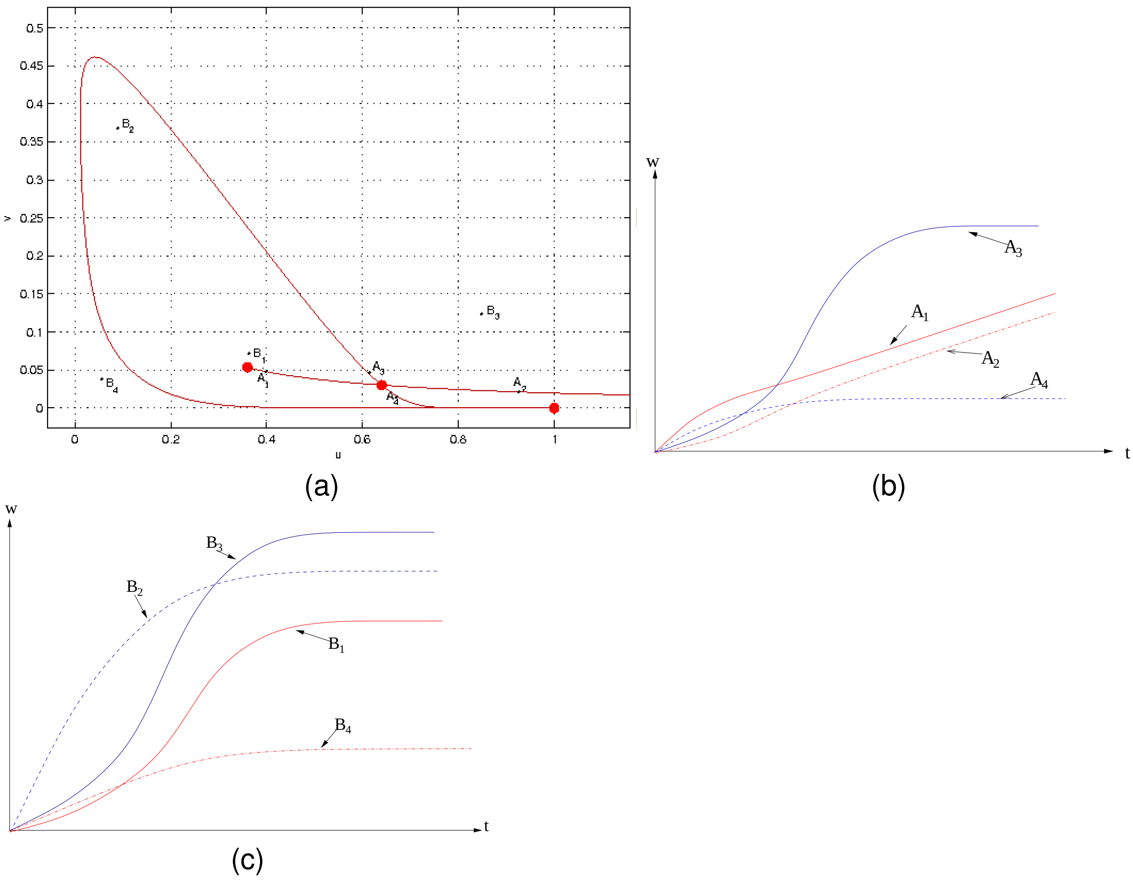

Figure 11: (a): some initial states in parameter region I which lie on stable and unstable trajectories at S_3 and some other initial states. Growth forms corresponding to initial states (b) A_1, A_2, A_3, A_4 and (c) B_1, B_2, B_3 and B_4.

via stable trajectories of S_3 we can expect a uniform growth of coral. However, if the system comes to stabilization S_1 we can't expect a growth of the solid after stabilization. Different initial states and corresponding growth forms of solid material are shown in Figure (11). Each growth forms are labled by the corresponding initial state. Some initial states (A_1, A_2, A_3, A_4, B_1, B_2, B_3 and B_4) in parameter region I and corresponding growth forms are shown in Figure (11). Continuous growth of corals can be occurred only if the initial state lies on the stable trajectories at S_3 (After the trajectory reach S_3 a uniform growth of coral can be expected). In all other cases corals grow until the trajectory reaches to S_1 and after that no growth occurs.

The qualitative growth forms in parameter regions I and II are same (may be different in quantitatively) except the cases that the initial state very close to S_2. If the initial states lie near to S_2 in parameter region I and II, the growth forms of solid are shown in Figure (12).

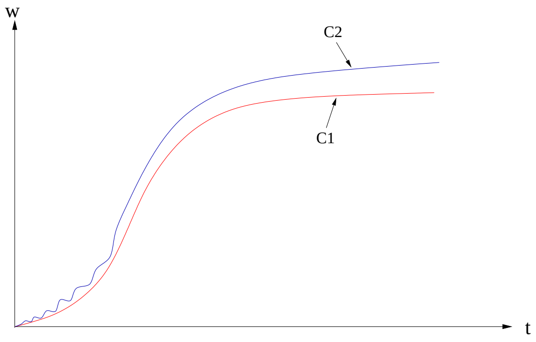

Figure 12: Growth forms when the initial state lies near S_2. $C1$ and $C2$ denote the growth forms when the initial state lies near S_2 in region I and II respectively

4.2 Heterioclinic connections and phase diagrams in parameter region III and IV

Since S_1, S_2 and S_3 are stable node, stable spiral and saddle respectively in parameter region III, a trajectory entering into the region $\mathcal{R}$, approaches to S_1 , S_2, S_3(only through the two stable trajectories) or a limit cycle. Similarly, Since S_3 is a saddle and S_2 and S_1 are stable nodes in region IV, a trajectory entering in to the region $\mathcal{R}$ approaches to S_1, S_2, S_3(only through the two stable trajectories) or a limit cycle.

Theorem 4.3. *For α and λ in regions III(sufficiently away from Hopf bifurcation) and in region IV there are two heterioclinic connections between S_3 and S_1.*

Proof. Since, in this case the steady state S_2 is stable(stable spirals in region III, stable nodes in region IV) the unstable trajectories emerging from S_3 should reach to S_2 or S_1. □

The behaviors of the heteroclinic connections for particular parameter values in regions III and IV are shown in Figure (13). The behaviors of the trajectories in parameter region III and IV for particular parameter values are shown in Figure (14).

4.3 Seperatrixes

The phase diagrams in Figures (14) show that all the trajectories above the stable trajectories of S_3 reach the steady state S_2 and all the trajectories below the stable trajectories of S_3 reach the steady state S_1. That is, the stable trajectories of S_3 act as seperatrix. Since any trajectory starting at a point above the seperatrix reaches S_2, a uniform growth of solid can be expected after the system reaches S_2. Also, any trajectory starting at a point on the seperatrix reaches S_3. Hence a uniform growth of solid can be expected after the system comes to stabilization. Since $v_{s2} > v_{s3}$ the growth rate of condensing solid materials in latter case is lower than that of previous case. On the other hand, any trajectory starting at a point below to the seperatrix reaches S_1, and hence there is no growth of the solid after the system comes to stabilization. In brief there are two uniformly growing states of condensed solid if the system comes to the steady states S_2 or S_3 and no growth of condensed solid if the system comes to steady state S_1. Different initial states and corresponding growth forms of solid material (coral) are shown in Figure (15). The growth forms in region IV is almost similar (may be different quantitatively) to the growth forms in region III except the growth forms near S_2. By these observations, it can be concluded that if someone expect a continuous growth of corals in a tank, the system should be adjusted such that the initial state lies above the seperatrix.

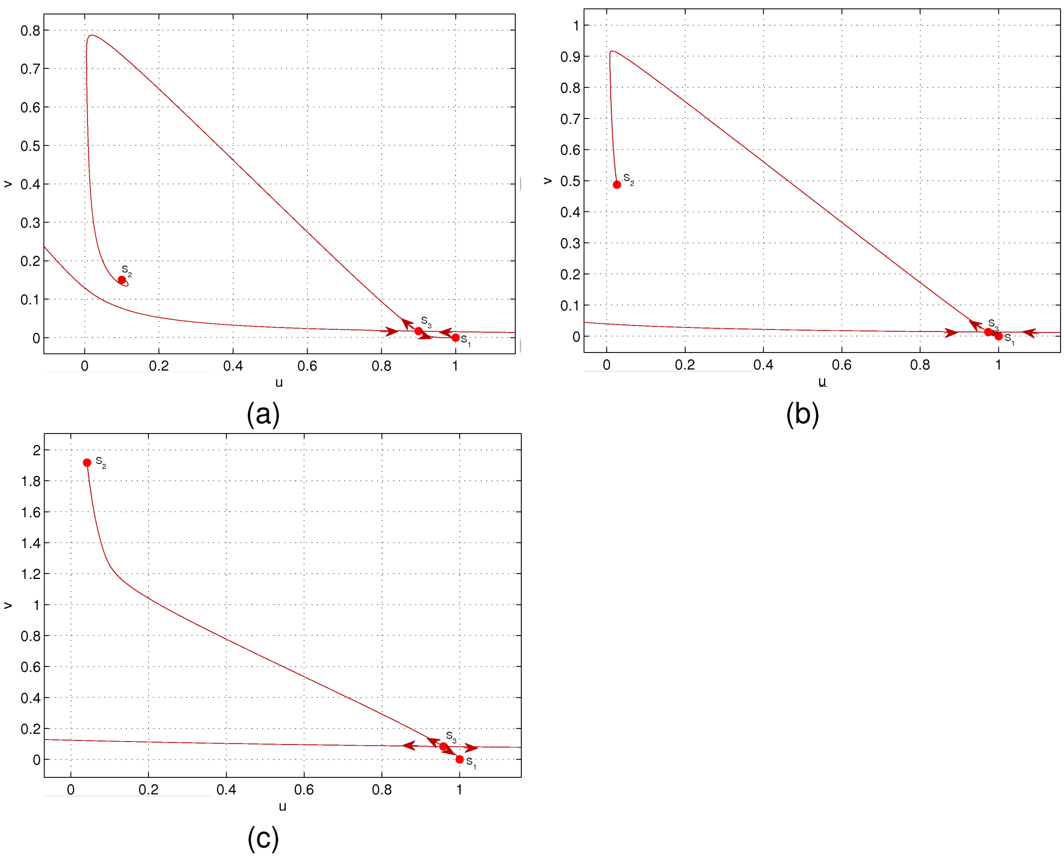

Figure 13: Stable and unstable trajectories starting at S_3 in parameter region: (a) III for $\alpha = 20$, $\lambda = 6$; (b) IV for $\alpha = 12.5$, $\lambda = 2.0$, and (c) IV for $\alpha = 2.4$, $\lambda = 0.5$.

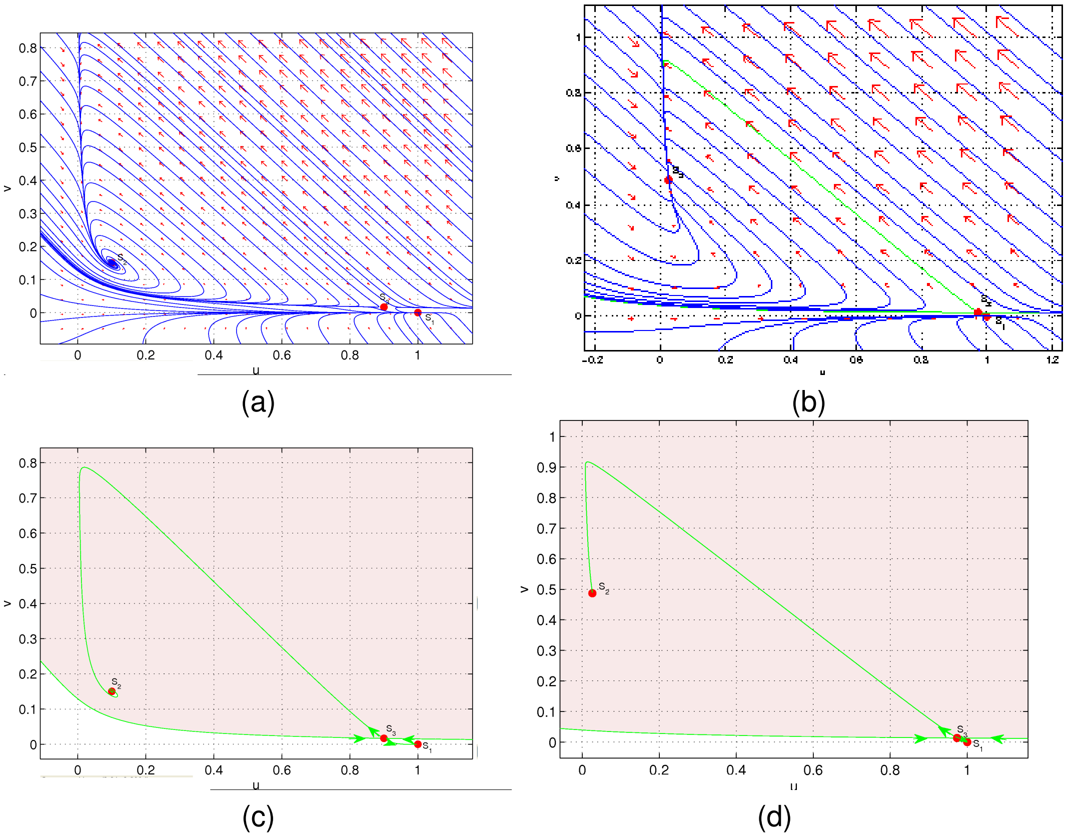

Figure 14: Phase plane diagrams in: (a) region III for $\lambda = 6$, $\alpha = 20$;(b)region IV for $\lambda = 2$, $\alpha = 12.5$. Domain of attraction (Shaded areas) of S_1 in regions: (c) III for $\lambda = 6$, $\alpha = 20$ and (d) IV for $\lambda = 2$, $\alpha = 12.5$.

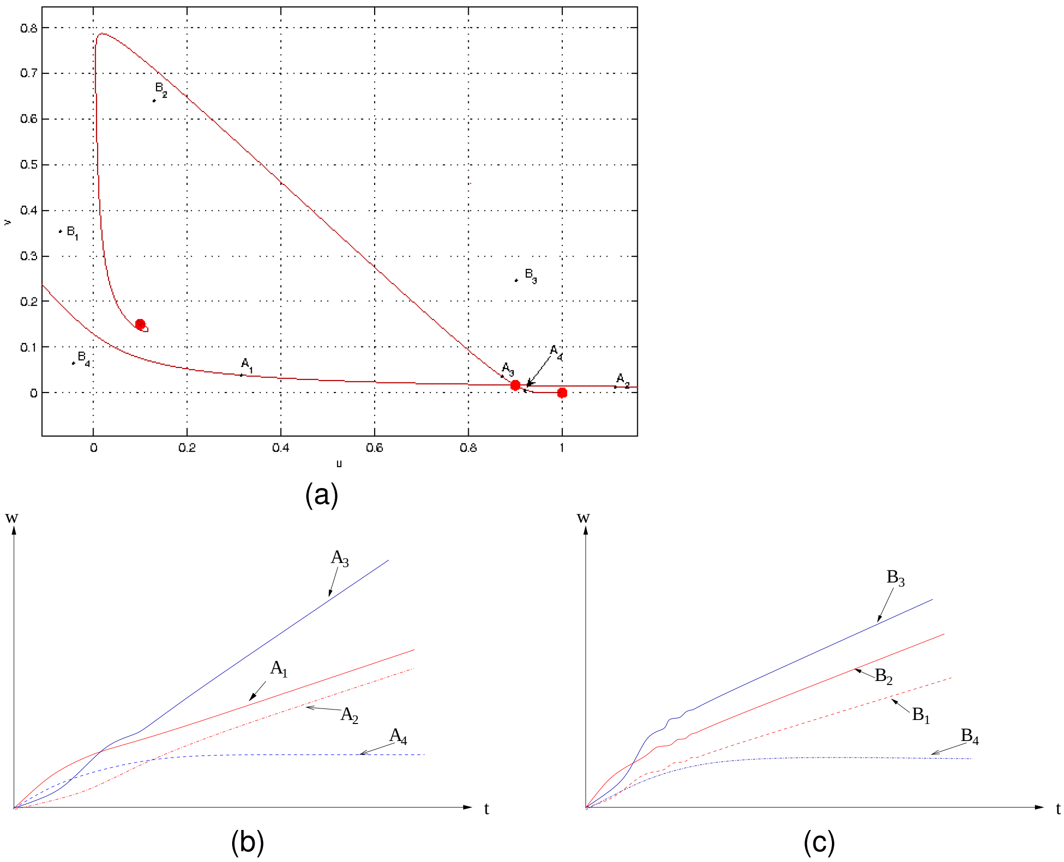

Figure 15: (a) Some initial states in the parameter region III which are lying on the stable and unstable trajectories at S_3 and on some other initial states. Growth forms corresponding to initial states: (b) A_1, A_2, A_3, A_4 and (c) B_1, B_2, B_3 and B_4.

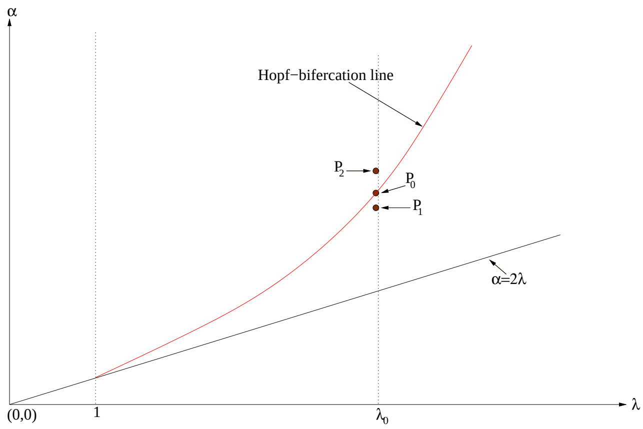

Figure 16: Three points in a neighborhood of Hopf-bifurcation line

4.4 Existence of oscillatory solutions

It is observed that Δ_2 is negative in regions II and III. That is there exist imaginary parts in the corresponding eigenvalues. Therefore there exist local oscillatory solutions for the system of ordinary differential equations (3.1), about S_2.

4.4.1 Stable and unstable trajectories and phase diagrams about a neighborhood of Hopf bifurcation line

The three different points P_0, P_1 and P_2 that we have considered (see Figure (16)) in the parameter space lie in a neighborhood of the Hopf bifurcation line. Let $P_0 = \left(\lambda_0, \dfrac{\lambda_0^2}{\sqrt{\lambda_0 - 1}}\right)$, be a point on the Hopf-bifurcation line. Let $P_1 = \left(\lambda_0, \dfrac{\lambda_0^2}{\sqrt{\lambda_0 - 1}} - \delta\right)$ and $P_2 = \left(\lambda_0, \dfrac{\lambda_0^2}{\sqrt{\lambda_0 - 1}} + \delta\right)$ be two points which lie in regions II and III respectively. Here, $\lambda_0 > 1$ and $\delta << 1$. Now we consider the behavior of the trajectories and hence growth forms of solid correspond to the parameter points P_0, P_1 and P_2 respectively:

At parameter point P_0: The stable and unstable trajectories at S_3 that correspond to $\lambda_0 = 3.5$, are shown in Figure (17)(a). One of the unstable trajectories reaches S_1 and other one spirally reaches a point on a closed curve, which is one of the centers about S_2(see Figure (17)(a)). Phase plane diagram corresponding to parameter point P_0 is shown in Figure (17)(b).

In this case, stable trajectories of S_3 act as seperatrix. All the trajectories lying above the seperatrix reach S_2 and all the trajectories lying on seperatrix reach S_1. So we can expect a damping periodical growth of the solid until the system comes to stabilization. After that, the growth is uniform corresponding to any initial state which lie above the seperatrix. Also, if the initial state lies on the seperatrix, one can expect uniform growth of coral after stabilizing at S_3. If the initial state lies at a point below the seperatrix, there is no growth after the stabilization of the system at S_1(see Figure (18)).

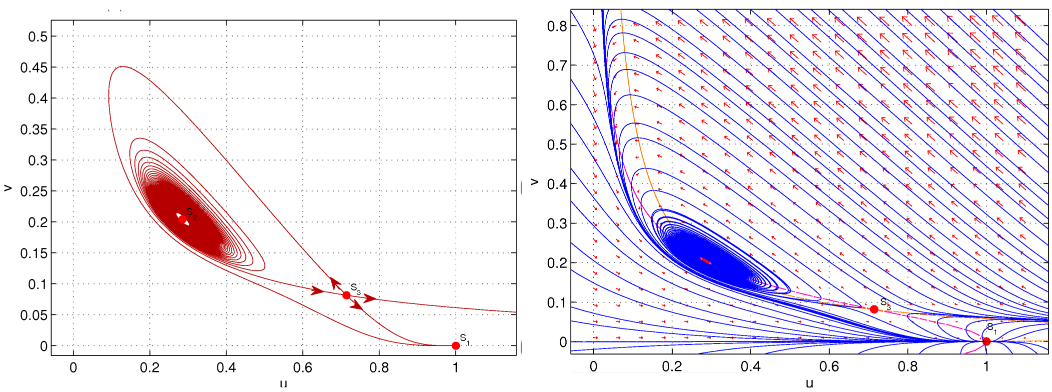

(a) (b)

Figure 17: (a) Stable and unstable trajectories starting at S_3 and (b) phase plane diagram corresponding to parameter point P_0 for $\lambda_0 = 3.5$

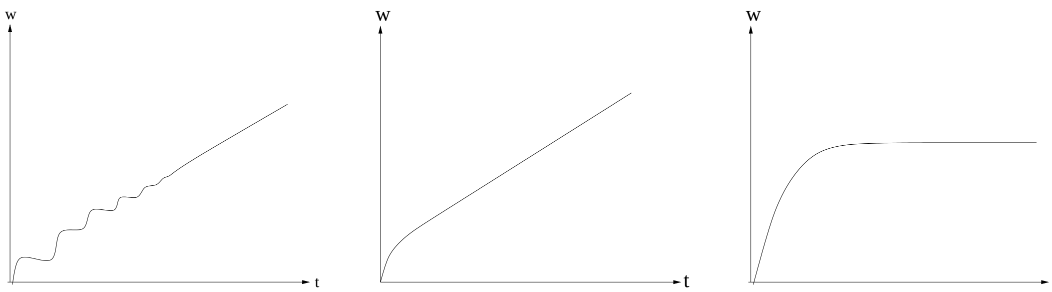

(a) (b) (c)

Figure 18: Growth forms at parameter point P_0 when the initial state lies: (a) above the seperatrix (b) on the seperatrix (c) below the seperatrix.

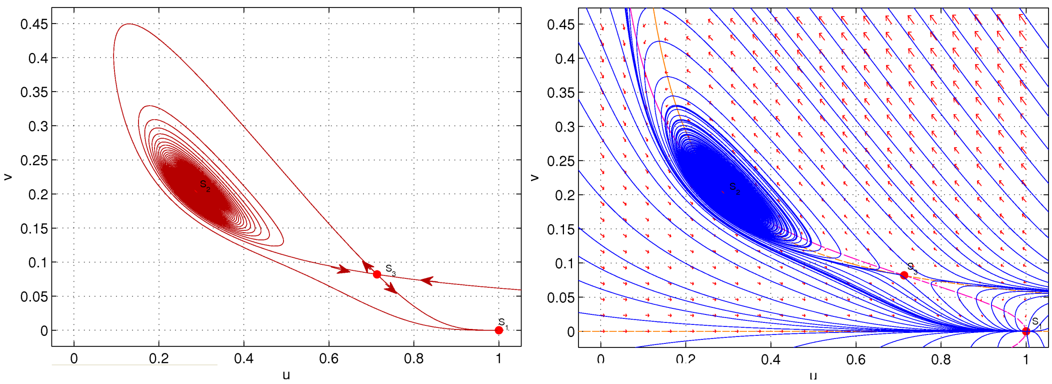

(a) (b)

Figure 19: (a) stable and unstable trajectories starting at S_3 and (b) phase plane diagram; corresponding to parameter point P_1, for $\lambda_0 = 3.5$, $\delta = 0.009$

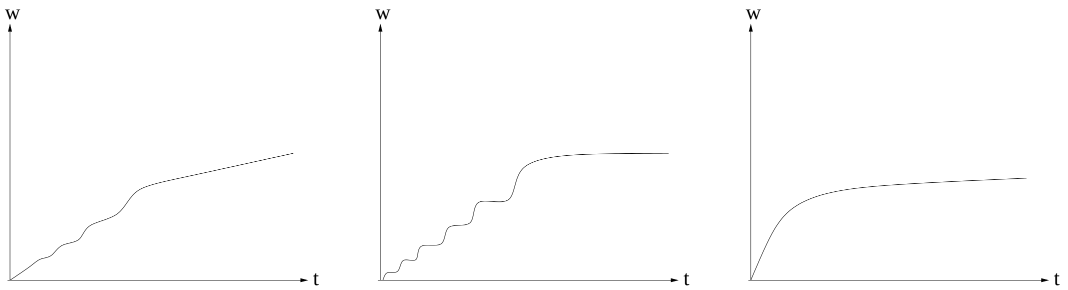

(a) (b) (c)

Figure 20: Growth forms at P_1 when initial state lies: (a) on the stable trajectory of S_3, which starts at S_2 (b) near the S_2 which doesn't lie on stable trajectory of S_3 (c) sufficiently away from S_2

At parameter point P_1: The stable and unstable trajectories at S_3 corresponding to the parameter points P_1, for $\lambda_0 = 3.5$, $\delta = 0.009$ are shown in Figure (19)(a).

At the parameter point P_1, unstable trajectories of S_3 reach S_1 in two different paths (two heteroclinic connections between S_3 and S_1). One of the stable trajectories at S_3 emerges from S_2. That is there is a heteroclinic connection between S_2 and S_3. The phase plane diagram corresponding to parameter point P_1 is shown in Figure (19)(b).

In this case, S_2 is a spiral source and all the trajectories, except the stable trajectories of S_3 reach S_1. Therefore, uniform growth state of condensed solid can be expected only through stable trajectories of S_3. See Figure (20) for different growth forms for different initial states.

At parameter point P_2: The stable and unstable trajectories at S_3 corresponding to the parameter points P_2, for $\lambda_0 = 3.5$, $\delta = 0.009$ are shown in Figures (21). According to this figure, at the parameter point P_2, stable trajectories of S_3 reaches S_1 in two different paths (Two heteroclinic connections between S_3 and S_1) as at point P_1. On the other hand, in this case, one of the stable trajectories is originating from a point on a closed curve about S_2. In other words, there is an unstable limit cycle

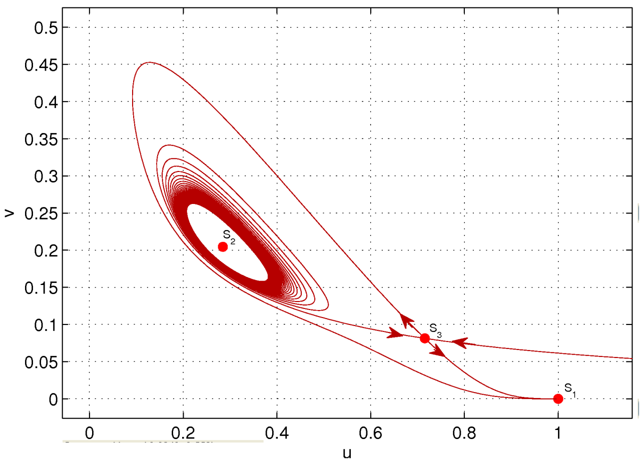

Figure 21: Stable and unstable trajectories of S_3 corresponding to parameter point P_2, for $\lambda_0 = 3.5$, $\delta = 0.009$

about S_2.

Phase plane diagram corresponding to parameter point P_2 is shown in Figure (22)(a). In this case, S_2 is a spiral sink and all the trajectories on the phase plane, except the stable trajectories of S_3 and the trajectories inside of the limit cycle, tend to S_1. Since S_2 is a spiral sink all the trajectories inside the limit cycle, reach to S_2 itself (See Figure (22)(b)). In other words, if the initial state lies inside the limit cycle, there are damping oscillatory solutions for u and v that are stabilizing at S_2. In this case, a damping oscillatory growth of condensed solid (coral) can be expected at the beginning and as time passes (after stabilizing), a uniform growth of condensed solid (coral) can be expected. See Figure (23) for different growth forms for different initial states.

4.5 Existence of limit cycles

Let $\mu =$ Re$\mu \pm$ Imμ be eigenvalues of the linearized system about the equilibrium point (u_{s2}, v_{s2}). On the line $\alpha = (p_2)\alpha_1 = \frac{\lambda^2}{\sqrt{\lambda - 1}}$, Re$(\mu(\alpha, \lambda)) = 0$ and Im$(\mu(\alpha, \lambda)) \neq 0$. In region II, Re$(\mu(\alpha, \lambda)) > 0$ and in Region III, Re$\mu(\alpha, \lambda) < 0$. Then according to [Murray (2003)](p. 221) in a small neighborhood of $\alpha = (p_2)\alpha_1 = \frac{\lambda^2}{\sqrt{\lambda - 1}}$, which lies in region II, the steady state is unstable due to growing oscillations and at least, small amplitude limit cycle periodic solution should exist about S_2. The period of this limit cycle solution is given by $2\pi/\omega$ where $\omega = Im(\mu((p_2)\alpha_1, \lambda))$.

4.5.1 Limit cycles in the Region III

The conditions of the eigenvalue method for the limit cycles hold at the points near the curve $\alpha = (p_2)\alpha_1$ which lie in the region III. Stable and unstable trajectories at S_3 at the parameter point $((p_2)\alpha_1 + \delta, \lambda)$ for $\lambda = 3.5$ and for different values of δ are shown in Figure (24). A growth of unstable limit cycles can be observed as δ increases up to some critical value (say $\delta_c(\lambda)$) and also limit cycles vanish when $\delta > \delta_c(\lambda)$. Also, one can guess that, when $\delta = \delta_c(\lambda)$ the unstable limit cycle at S_3 reaches S_3 itself. That is, one of the heteroclinic connection between S_3 and S_1 becomes a homoclinic connection at

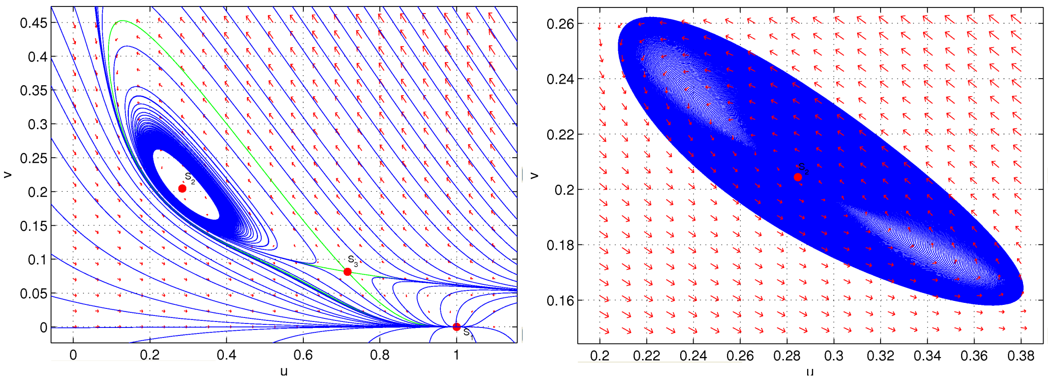

(a) (b)

Figure 22: (a) Phase plane diagram corresponding to parameter point P_2 for $\lambda_0 = 3.5$, $\delta = 0.009$ (b) Phase plane diagram in a small neighborhood of S_2 correspond to same parameter values

S_3 when δ increases to δ_c. This homoclinic connection is shown in Figure (25). It is observed (by numerical experiments) that $\delta_c(3.5) \approx 0.098$.

4.5.2 Growth forms corresponding to initial state lie inside and out sides of the limit cycle

Now consider a point A which lie inside of the limit cycle and two points B and C which lie outside of the limit cycle (see Figure (26)). Here B is a point on a stable trajectory of S_3 and C does not lie on that stable trajectory. Growth forms of the solid when initial state lies at A, B and C are shown in Figure (27). If the initial state lies inside the limit cycle, we can expect a damping oscillatory growth until the system stabilize at S_2. After that we can expect a uniform growth. If the initial state lies outside the limit cycle, continuous growth of solid cannot be expected. In this case, it grows until the system stabilize at S_1 and after that cease the growth. Also, continuous growth can be expected if the initial state lies on the stable trajectories of S_3.

5 Discussion

Throughout this article it has been reasonably assumed that the parameters (α and λ) of the model are non-negative real constants. The phase plane diagrams used in this article are obtained by using the MATLAB program pplane [John (2011)]. According to the existing number of real steady states of the system, the parameter space can mainly be divided into three regions (see Table 2).

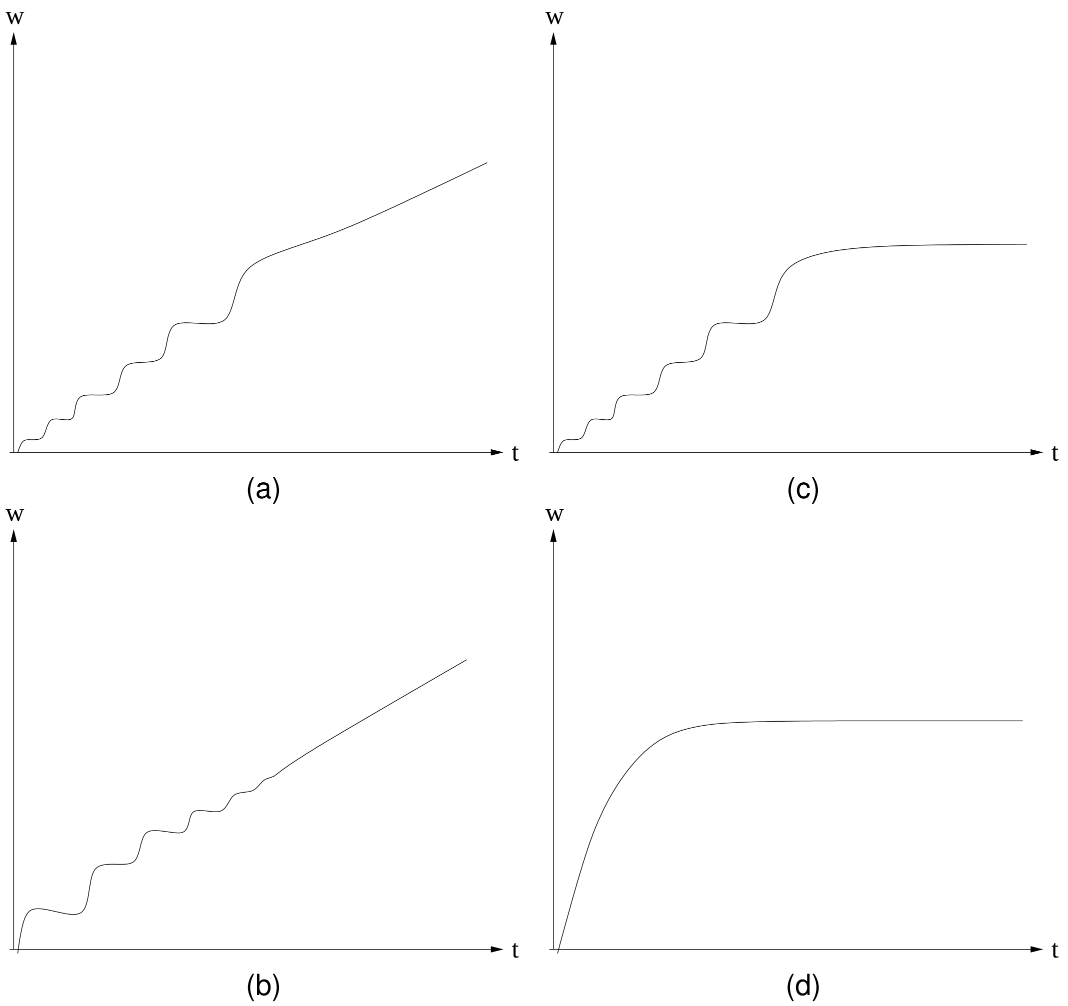

Figure 23: Growth forms at P_2 when the initial state lies (a) on a point of the stable trajectory of S_3 which starts at S_2 (b) at a point inside the limit cycle (c) at a point near the S_2 (Outside the limit cycle) which doesn't lie on stable trajectory of S_3 (d) at a point sufficiently away from S_2

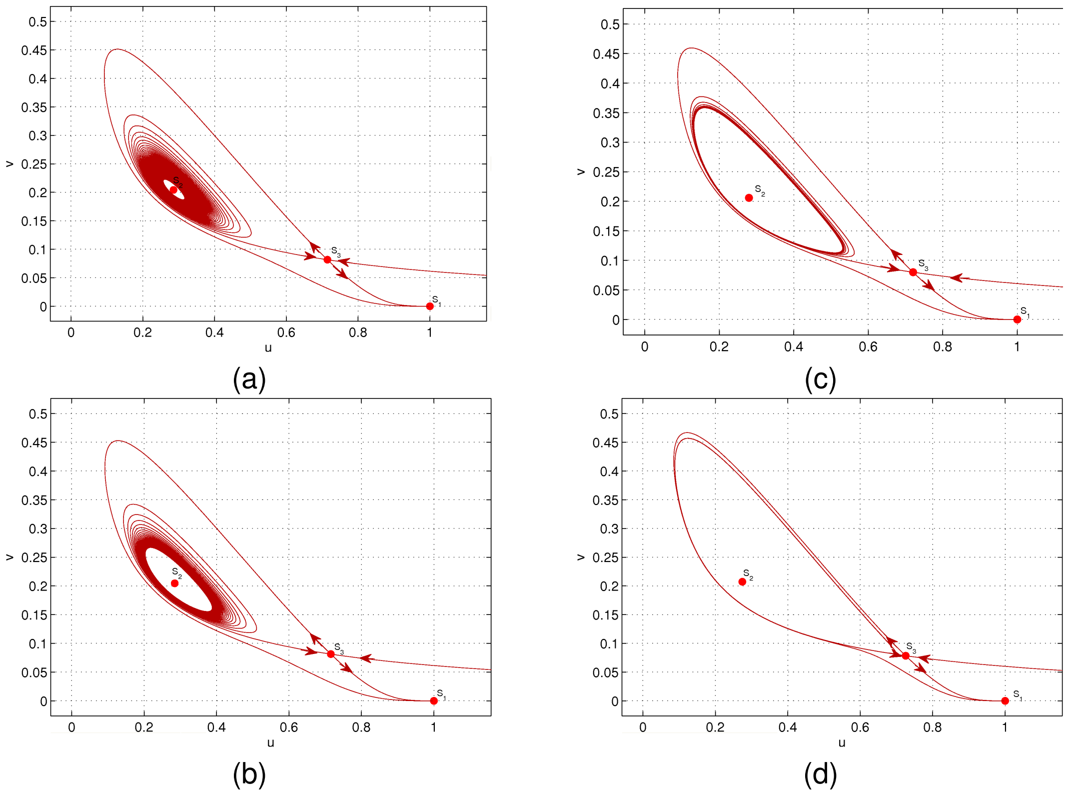

Figure 24: Stable and unstable trajectories at S_3 at parameter point $((p_2)\alpha_1 + \delta, \lambda)$ when $\lambda = 3.5$ for: (a) $\delta = 0.001$ (b) $\delta = 0.01$ (c) $\delta = 0.05$ and (d) $\delta = 0.095$

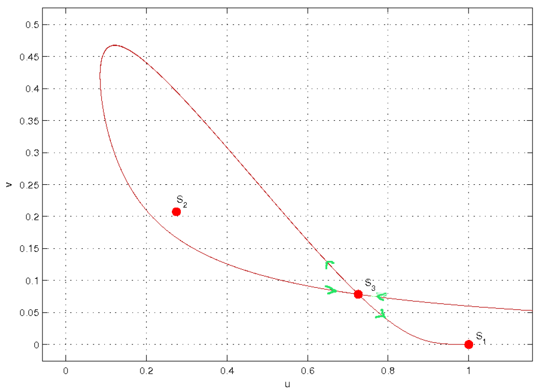

Figure 25: Homoclinic connection at S_3 for $\lambda = 3.5$, $\delta = \delta_c(3.5) = 0.098$

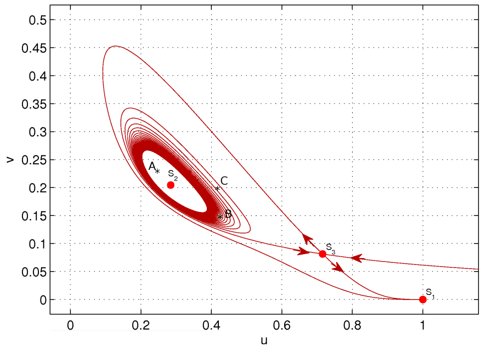

Figure 26: Three initial states inside and out side of the limit cycle.

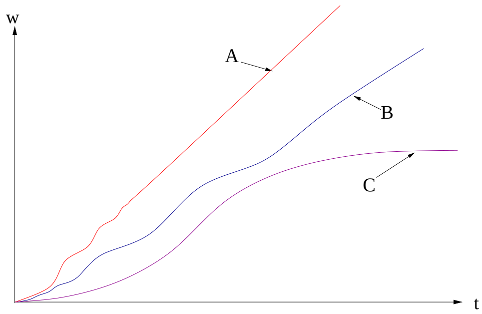

Figure 27: Growth forms corresponding to initial states A, B and C.

Region	No. of equalibria
Region A: $\alpha > 2\lambda$	3 (denoted S_1, S_2, S_3)
Region B: $\alpha = 2\lambda$	2 (denoted S_1, $S_2 \equiv S_3$)
Region C: $\alpha < 2\lambda$	1 (denoted S_1)

Table 2:

In this article, our main concern has been on the behavior of the solution of the system at parameter region A. In region A, S_1 is a stable node, S_3 is a saddle point and again the behavior of S_2 depends on the parameter values. According to the behavior of S_2, the region A can be divided into four subregions *region I*, *region II*, *region III* and *region IV*. In each subregion the behavior of S_2 is classified as shown in Table 3.

Subregion	Type of the equalibria S_2
I	Unstable nodes
II	Unstable spirals
III	Stable spirals
IV	Stable nodes

Table 3: Stability of S_2 in different parameter regions

It has been observed that, there is a confined set containing S_1, S_2 and S_3 in parameter region A. That is, all the trajectories converge to some point in this confined set. Also, it has been observed that there are three heteroclinic connections in subregions I and II, while two heteroclinic connections are in subregions III (sufficiently away from Hopf bifurcation) and IV. Growth forms of the solid are identified when the parameters lie in each parameter region for different initial states. Some of the identified growth forms are:

- Grow with decreasing rate up to some time (say τ_1) and no growth after that. In this case the system stabilizes at S_1 at time τ_1.

- Grow with increasing rate up to some time (say τ_2) and after that growth become uniform. In this case the system stabilizes at S_2 or S_3 at time τ_2.
- grow with oscillatory rate up to some time (say τ_3) and after that growth become uniform. In this case the system stabilizes at S_2 or S_3 at time τ_3.
- grow with oscillatory rate up to some time (say τ_4) and after that no growth occurs. In this case the system stabilizes at S_1.

Unstable limit cycles were observed when the parameters lie in region III very close to the Hopf bifurcation curve. Also, the growth forms of the coral are identified corresponding to different initial states when parameters lie in different parameter regions. Also, homoclinic connections at S_3 are observed for particular parameter values which lie in region III very close to the Hopf Bifurcation curve. Finally, continuous growth forms of the solid could be happened when parameters lie only in regions III and IV. Therefore, parameter regions III and IV are practically important.

The amount of the solid deposited within a particular time period depends on the parameter values, initial state and the v component of the steady state, (u_s, v_s). For example, consider the growth forms corresponding to $\alpha > 2\lambda$. Suppose that a trajectory in (u, v) plane starts from the initial state $\underline{\mathbf{u}}_0 \equiv (u_0, v_0)$ at $t = 0$ and that trajectory reaches the steady state (u_s, v_s) at $t = t_s$. Then the stabilizing period t_s, shall depend on $\underline{\mathbf{u}}_0$. Let w_s denote the deposit amount of solid material within the time period t_s. Then w_s depends on v_s as well as $\underline{\mathbf{u}}_0$. If $v_s \neq 0$ then the growth of solid depends on v_s.

Suppose that the system reaches a steady state S_2 or S_3. Then the solid material deposit uniformly in a rate proportional to v_s after $t = t_s$. For given λ, v_s increases from $1/(2\lambda)$ to $1/\lambda$ as α increases (see Figure (4)(b)). Therefore, for fixed λ the minimum and maximum values of the possible uniform growth rates of solid are proportional to $1/(2\lambda)$ and $1/\lambda$ respectively. This minimum and maximum growth rates are occurred at $\alpha = 2\lambda$ and $\alpha \to \infty$ respectively. Since $\alpha = \dfrac{k_1 u_s^2}{k}$ and $\lambda = \dfrac{k_2}{k}$, the minimum growth rate occur when $\dfrac{k_1}{k_2} = \dfrac{2}{u_s^2}$. For fixed k, k_2 and u_s the maximum growth rates occur when $k_1 \to \infty$. That is higher reaction rates of u and v cause to higher growth rates of corals when k and u_s are fixed.

Acknowledgment

Authors would like to thank unknown reviewers for their valuable suggestions and comments which were very much helpful to improve the quality of the paper.

Competing interests

The authors declare that they have no competing interests.

References

António F. Miguel. (2006). Constructal pattern formation in stony corals, bacterial colonies and plant roots under different hydrodynamics conditions Journal of Theoretical Biology 242(4), 954-961.

Castro, P., Huber, M.E. 1997 Marine Biology WCB/McGraw-Hill

Coralscience (2012), http://www.coralscience.org/main/articles/development-5/modelling-coral-growth. *(Last accessed on 23 May 2012).*

Encyclopedia (2012) Coral growth and climate change. Encyclopedia of Earth. Eds. Cutler J. Cleveland (Washington, D.C.: Environmental Information Coalition, National Council for Science and the Environment). [First published in the Encyclopedia of Earth March 30, 2010; Last revised Date May 7, 2012; http://www.eoearth.org/article/Coral_growth_and_climate_change*(Last accessed on 23 May 2012)*.

John C. Polking (2011), PPlane (MATLAB program for phase plane analysis), http://math.rice.edu/ dfield/dfpp.html *(Last accessed on 17 May 2011)*.

Jordan D.W. and Smith P. (1987) Nonlinear Ordinary Differential Equations Oxford University press, New York (Second edition).

Kaandorp J.A. et al. (1996) Effect of Nutrient Diffusion and Flow on Coral Morphology, Physical Review Letters 77 (11) 2328-2331.

Kaandorp J.A. et al. (2005) Morphogenesis of the branching reef coral Madracis mirabilis Proc. R. Soc. B 272, 127133.

Kaandorp J.A. et al. (2008) Modelling genetic regulation of growth and form in a branching sponge Proc. R. Soc. B 275, 25692575.

Kruszyjski, K.J. Kaandorp, J.A. Liere, R.V. (2006) A computational method for quantifying morphological variation in scleractinian corals Coral Reefs DOI 10.1007/s00338-007-0270-6 .

Maxim, V. F. et al. (2010) A comparison between coral colonies of the genus Madracis and simulated forms Proc. R. Soc. B 277, 35553561.

Merks, R. M. H. (2003a). Branching grwth in Stony Corals *a modelling approach* Advaced School of Computing and Imaging, University of Amsterdam *PhD Thesis*.

Merks R. M. H. (2003b). Models of coral growth: Spontaneous branching, compactification and Laplacian growth assumption Journal of Theoretical Biology .

Merks R. M. H. (2003c). Diffusion-limited Aggregation in Laminar Flows International journal of Modern Physics C 14,(9), 1171-1182.

Mistr, S. and Bercovici D. (2003). A theoretical Model of Pattern Formation in Coral Reefs Ecosystems 6 61-74.

Murray J.D. (2003) Mathematical Biology: An Introduction Springer-Verlag Berlin Heidelberg Volume I.

Osinga, R. et al. (2011) The Biology and Economics of Coral Growth. Mar. Biotechnol (13), 658-671.

Marineeducation (2012),http://www.usm.edu/marineeducation/old/coralreef/03.pdf. *(Last accessed on 23 May 2012)*.

Peer-review history:
The peer review history for this paper can be accessed here (Please copy paste the total link in your browser address bar)
www.sciencedomain.org/review-history.php?iid=165&id=6&aid=772